Intracellular TRPA1 mediates Ca^{2+} release from lysosomes in dorsal root ganglion neurons

Shujiang Shang,[1,2,3]* Feipeng Zhu,[1]* Bin Liu,[1]* Zuying Chai,[1] Qihui Wu,[1] Meiqin Hu,[1] Yuan Wang,[1] Rong Huang,[1] Xiaoyu Zhang,[1] Xi Wu,[1] Lei Sun,[1] Yeshi Wang,[1] Li Wang,[1] Huadong Xu,[1] Sasa Teng,[1] Bing Liu,[1] Lianghong Zheng,[1] Chen Zhang,[3] Fukang Zhang,[4] Xinghua Feng,[5] Desheng Zhu,[2] Changhe Wang,[1] Tao Liu,[1] Michael X. Zhu,[5] and Zhuan Zhou[1]

[1]State Key Laboratory of Membrane Biology and Beijing Key Laboratory of Cardiometabolic Molecular Medicine, Institute of Molecular Medicine and Peking-Tsinghua Center for Life Sciences and PKU-IDG/McGovern Institute for Brain Research, [2]Laboratory Animal Center, and [3]School of Life Science, Peking University, Beijing 100871, China
[4]Institute for Biomedical Science of Pain, Capital Medical University, Beijing 100069, China
[5]Department of Integrative Biology and Pharmacology, The University of Texas Health Science Center at Houston, Houston, TX 77030

Transient receptor potential A1 (TRPA1) is a nonselective cation channel implicated in thermosensation and inflammatory pain. In this study, we show that TRPA1 (activated by allyl isothiocyanate, acrolein, and 4-hydroxynonenal) elevates the intracellular Ca^{2+} concentration ($[Ca^{2+}]_i$) in dorsal root ganglion (DRG) neurons in the presence and absence of extracellular Ca^{2+}. Pharmacological and immunocytochemical analyses revealed the presence of TRPA1 channels both on the plasma membrane and in endolysosomes. Confocal line-scan imaging demonstrated Ca^{2+} signals elicited from individual endolysosomes ("lysosome Ca^{2+} sparks") by TRPA1 activation. In physiological solutions, the TRPA1-mediated endolysosomal Ca^{2+} release contributed to ∼40% of the overall $[Ca^{2+}]_i$ rise and directly triggered vesicle exocytosis and calcitonin gene-related peptide release, which greatly enhanced the excitability of DRG neurons. Thus, in addition to working via Ca^{2+} influx, TRPA1 channels trigger vesicle release in sensory neurons by releasing Ca^{2+} from lysosome-like organelles.

Introduction

The transient receptor potential (TRP) superfamily is composed of a large number of cation channels with diverse functions and expression patterns in mammalian systems (Wu et al., 2010; Montell, 2011). TRPA1 is the sole member of the TRPA subfamily in mammals. It is highly expressed in a subset of primary sensory neurons in the dorsal root and trigeminal ganglia that are known to function in nociception (Story et al., 2003; Jordt et al., 2004). TRPA1 channels are selectively activated by various pungent chemicals, environmental irritants, and endogenous ligands, including mustard oil (allyl isothiocyanate [AITC]), acrolein, and 4-hydroxynonenal (4-HNE; Bandell et al., 2004; Bautista et al., 2006; Trevisani et al., 2007; Andersson et al., 2008; Ruparel et al., 2008; Karashima et al., 2009; Hu et al., 2010). Furthermore, inflammatory factors such as bradykinin indirectly activate TRPA1 channels by activating PLC (Bandell et al., 2004). This uniquely broad agonist profile along with its regulatory properties make it possible for the TRPA1 channel to function in thermosensation, environment-irritant sensing, and nociceptive sensation (Story et al., 2003; Bandell et al., 2004; Bautista et al., 2006; Kwan et al., 2006; Macpherson et al., 2007; McNamara et al., 2007).

The TRPA1 channel has been shown to function on the plasma membrane, and nociceptive signals induce its translocation from a cytosolic pool to the plasma membrane (Bautista et al., 2006; Schmidt et al., 2009). TRPA1 channel activation increases sensory neuron excitability and the intracellular Ca^{2+} concentration ($[Ca^{2+}]_i$; Jordt et al., 2004). It has been shown that ∼17% of the TRPA1 current is mediated by Ca^{2+} influx (Karashima et al., 2010). In contrast to the extensive studies of TRPA1 activators/modulators and the mechanisms of regulation in heterologous expression systems, the regulation and sources of the TRPA1-induced Ca^{2+} signal in dorsal root ganglion (DRG) neurons and other native cells remain largely unknown. In this study, we systematically investigated the Ca^{2+} signal

*S. Shang, F. Zhu, and B. Liu contributed equally to this paper.

Correspondence to Zhuan Zhou: zzhou@pku.edu.cn; Michael X. Zhu: michael.x.zhu@uth.tmc.edu; Tao Liu: tao.liu06@gmail.com; or Changhe Wang: changhewang@pku.edu.cn

Abbreviations used: 4-HNE, 4-hydroxynonenal; AITC, allyl isothiocyanate; ANOVA, analysis of variance; $[Ca^{2+}]_i$, intracellular Ca^{2+} concentration; CGRP, calcitonin gene-related peptide; C_m, membrane capacitance; CPA, cyclopiazonic acid; DRG, dorsal root ganglion; EIA, enzyme immunometric assay; FCCP, carbonylcyanide-p-(trifluoromethoxy)-phenylhydrazone; $[Fura\text{-}2]_i$, intracellular Fura-2 concentration; G_m, membrane conductance; GPN, glycylphenylalanine 2-naphthylamide; G_s, series conductance; KO, knockout; LAMP1, lysosome-associated membrane protein 1; NPY, neuropeptide Y; P_{store}, fractional contribution of the Ca^{2+} store; RR, ruthenium red; TG, thapsigargin; TIRF, total internal reflection fluorescence; TRPA1, transient receptor potential A1; VAMP2, vesicle-associated membrane protein 2; WT, wild-type.

The Rockefeller University Press $30.00
J. Cell Biol. Vol. 215 No. 3 369–381
https://doi.org/10.1083/jcb.201603081

triggered by TRPA1 activation, the mechanisms by which it regulates neuropeptide secretion in mouse DRG neurons, and its relevance to nociceptive sensation.

Results

Activation of TRPA1 channel mediates Ca^{2+} release from intracellular stores

Although the critical roles of TRPA1 channels in thermosensation, nociception, and environmental-irritant sensing are well known, details about the mechanisms of the TRPA1-mediated $[Ca^{2+}]_i$ rise in DRG neurons remained to be elucidated. We therefore monitored $[Ca^{2+}]_i$ changes in mouse DRG neurons stimulated with a TRPA1 agonist, AITC. Low concentrations of AITC are specific for TRPA1 (Bautista et al., 2006; Everaerts et al., 2011), whereas high concentrations (>0.1 mM) may activate TRPV1 as well (Everaerts et al., 2011). To ensure that 100 µM AITC, which was used for all of the cellular experiments, specifically activates TRPA1 in DRG neurons, we performed confocal microscopic Ca^{2+} imaging for unbiased screening of AITC-responsive DRG neurons in wild-type (WT) and TRPA1-knockout (KO) mice. Consistent with findings that only a subset of small-diameter DRG neurons express TRPA1 channels (Story et al., 2003), AITC (100 µM) induced a $[Ca^{2+}]_i$ rise in 33.5% of Fluo-4–loaded DRG neurons from WT, but not TRPA1-KO, mice (Fig. S1 A). Furthermore, the AITC-induced $[Ca^{2+}]_i$ rise remained largely unchanged in TRPV1-KO neurons, indicating that TRPV1 was not involved in the AITC responses in DRG neurons under our experimental conditions (unpublished data). We then quantified the TRPA1-mediated $[Ca^{2+}]_i$ rise in Fura-2–loaded neurons by photometric measurements (one cell per measurement). To avoid the desensitization of TRPA1 channels, we first screened for TRPA1-positive DRG neurons by Ca^{2+} imaging using a low concentration (25 µM) of AITC. Those that responded were chosen for subsequent experimental tests. Under these conditions, the $[Ca^{2+}]_i$ rise evoked in WT DRG neurons by 100 µM AITC was completely blocked by the specific TRPA1 antagonists HC-030031 and A-967079 (Fig. S2, A and B). The endogenous TRPA1 agonist acrolein (Bautista et al., 2006; Due et al., 2014) also induced a $[Ca^{2+}]_i$ increase in WT DRG neurons (Fig. S2 D). In contrast, neither AITC nor acrolein induced any change in $[Ca^{2+}]_i$ in TRPA1-KO neurons despite the robust response to capsaicin, a TRPV1 agonist (Fig. S2, C and D). These findings demonstrated that under our experimental conditions, AITC and acrolein induced a $[Ca^{2+}]_i$ rise by activating TRPA1 channels in DRG neurons.

TRPA1 is commonly thought to form plasma membrane channels that mediate Ca^{2+} influx. Surprisingly, application of 100 µM AITC in a Ca^{2+}-free (0 mM) external solution also led to a $[Ca^{2+}]_i$ rise in most of the capsaicin-sensitive WT DRG neurons, whereas little $[Ca^{2+}]_i$ change was detected in neurons pretreated with A-967079 (Fig. S3, A and B) or in those from TRPA1-KO mice (Fig. 1, A and B). Similarly, acrolein (Fig. S3, C and D) and another endogenous TRPA1 agonist, 4-HNE (Fig. S1 B; Trevisani et al., 2007; Andersson et al., 2008; Akude et al., 2010; Lupachyk et al., 2011), also triggered a $[Ca^{2+}]_i$ rise in WT, but not TRPA1-KO, DRG neurons in the Ca^{2+}-free external solution. The $[Ca^{2+}]_i$ rise should be completely contributed by intracellular Ca^{2+} sources because 1 mM EGTA was also included in the Ca^{2+}-free bath solution, and 100 mM K^+ failed to trigger any $[Ca^{2+}]_i$ rise under this condition (unpublished data). Furthermore, ∼30.4% of DRG neurons were still responsive to AITC in the Ca^{2+}-free condition with 2 mM BAPTA (Fig. 1, E and F), but were completely blocked by preloading with a membrane-permeable BAPTA-AM (Fig. 1, G and H). Thus, in addition to mediating Ca^{2+} influx through channels on the plasma membrane, activation of TRPA1 also mobilized Ca^{2+} from intracellular stores in DRG neurons. The AITC-induced Ca^{2+} store release was dependent on AITC concentration and saturable (Fig. 1, C and D). In AITC-positive DRG neurons bathed in the Ca^{2+}-free solution, application of AITC at 5, 20, 50, 100, and 300 µM caused increasing degrees of $[Ca^{2+}]_i$ elevation (Fig. 1, C and D). However, when DRG neurons were treated twice consecutively with 100 µM AITC in the Ca^{2+}-free solution, the second application failed to trigger a discernible $[Ca^{2+}]_i$ rise (unpublished data). These results indicated that the Ca^{2+} stores affected by TRPA1 activation were of a limited size and almost completely depleted by the first treatment with 100 µM AITC.

The ER is the major intracellular Ca^{2+} storage pool and responsible for most of the Ca^{2+} mobilization triggered by receptor signaling (Berridge, 2005). To investigate the possible involvement of the ER in mobilizing Ca^{2+} in response to TRPA1 activation, we first emptied the ER store by perfusion with Ca^{2+}-free external solution containing 2.5 µM thapsigargin (TG), a blocker of sarcoplasmic/ER Ca^{2+}/ATPases, before AITC was applied. However, this treatment did not notably change the AITC-induced release of stored Ca^{2+} (Fig. 2, A and B). Cyclopiazonic acid (CPA), another sarcoplasmic/ER Ca^{2+}/ATPase blocker, has been widely used to reversibly deplete the ER Ca^{2+} store (Seidler et al., 1989; Emptage et al., 2001). Similarly, preincubation of cells with Ca^{2+}-free solution containing 5 µM CPA also failed to affect the AITC-induced Ca^{2+} release (Fig. 2, C and D). Both TG and CPA triggered a $[Ca^{2+}]_i$ rise on their own because of Ca^{2+} leakage from the ER (Fig. 2, A and C). The Ca^{2+} ionophore ionomycin has been shown to preferentially target the ER membrane at low concentrations (up to 1 µM) but also affects other membranes at higher concentrations (e.g., 10 µM; Foyouzi-Youssefi et al., 2000). Therefore, we tested the effects of pre-emptying the internal stores with 1 or 10 µM ionomycin on AITC-induced Ca^{2+} release in DRG neurons. Both concentrations elicited a robust $[Ca^{2+}]_i$ rise when applied in the Ca^{2+}-free external solution. Consistently, 1 µM ionomycin failed to alter the effect of AITC on Ca^{2+} mobilization (Fig. 2 E), but 10 µM abolished the Ca^{2+} store release induced by TRPA1 activation (Fig. 2 F). These results demonstrated that the stores mobilized by TRPA1 activation did not reside in the ER.

Mitochondria are known to contain Ca^{2+} and participate in intracellular Ca^{2+} signaling (Brocard et al., 2001; Grienberger and Konnerth, 2012), so we next investigated whether mitochondria were involved in the Ca^{2+} mobilization in response to TRPA1 activation. Although the addition of carbonylcyanide-ρ-(trifluoromethoxy)-phenylhydrazone (FCCP; 3 µM), a mitochondrial proton gradient uncoupler that depletes the mitochondrial Ca^{2+} content (Brocard et al., 2001) in the Ca^{2+}-free solution caused a sustained $[Ca^{2+}]_i$ increase, it failed to affect the subsequent Ca^{2+} release in response to AITC (Fig. S3, E and F), indicating that mitochondria were not involved. A rise in $[Ca^{2+}]_i$ has been shown to activate exogenous TRPA1 channels located in the plasma membrane of HEK293 cells (Zurborg et al., 2007). However, Ca^{2+} release from the ER store induced by TG, CPA, and FCCP had no observable effect on the AITC-induced intracellular Ca^{2+} release in DRG neurons (Fig. 2 and Fig. S3, E and F), which might be because of the different recording

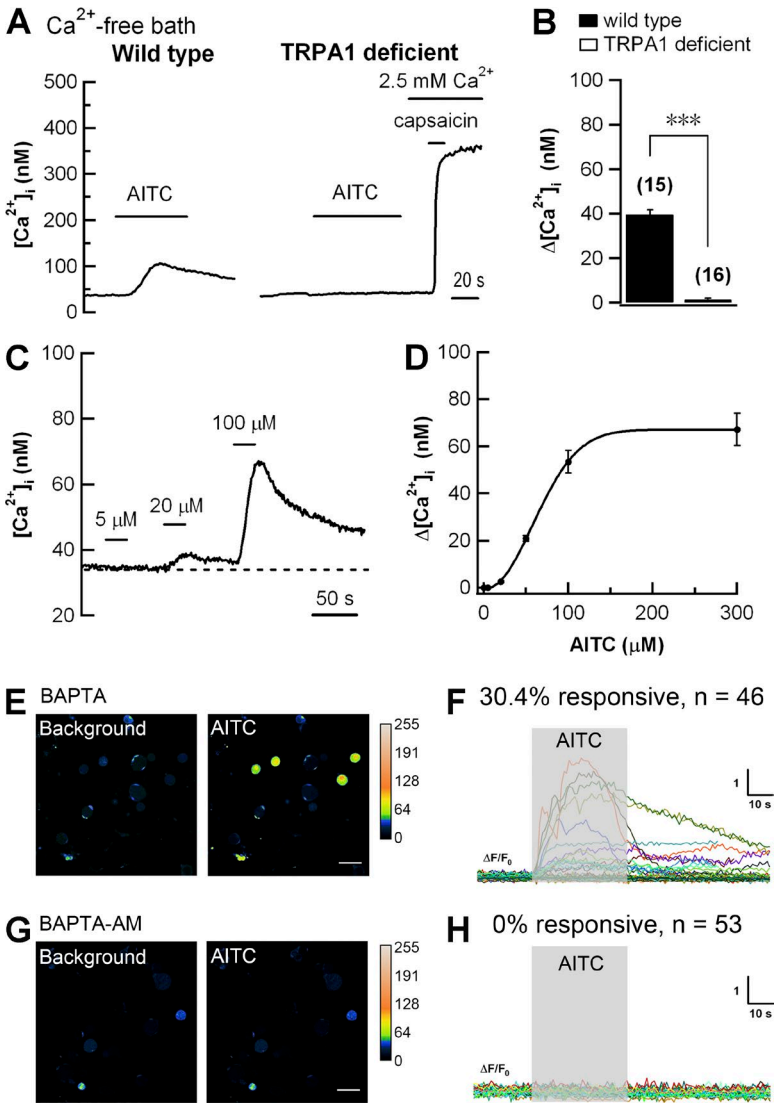

Figure 1. **TRPA1 channel activation triggers an intracellular Ca^{2+} rise in Ca^{2+}-free extracellular solution.** (A) Representative traces of AITC-induced $[Ca^{2+}]_i$ changes in DRG neurons from WT and TRPA1-KO mice in Ca^{2+}-free external solution. Extracellular Ca^{2+} was added, followed by capsaicin, to verify that the *TRPA1*$^{-/-}$ cell was a nociceptor. (B) Statistics of AITC-induced $[Ca^{2+}]_i$ changes in the Ca^{2+}-free solution (Student's *t* test, ***, $P < 0.001$). (C) $[Ca^{2+}]_i$ changes in a WT DRG neuron bathed in the Ca^{2+}-free solution in response to sequential applications of increasing concentrations of AITC. (D) Dose-response curve of AITC-induced $[Ca^{2+}]_i$ rises as in C. (E–H) Pseudocolor confocal images and fluorescence traces of Fluo4 showing that AITC induces $[Ca^{2+}]_i$ rises in 30.4% of DRG neurons in 2 mM BAPTA-containing Ca^{2+}-free extracellular solution (E and F), but not in neurons preloaded with 20 μM BAPTA-AM (G and H). Bars, 50 μm. Statistical data are presented as mean ± SEM, and *n* values in parentheses represent numbers of cells.

conditions or the different properties of exogenously expressed TRPA1 channels in HEK293 cells and the endogenous TRPA1 channels in DRG neurons.

TRPA1 channel activation mobilizes Ca^{2+} from lysosome-like organelles

Because secretory granules (i.e., secretory vesicles and lysosomes) have also been shown to contain Ca^{2+} and participate in intracellular Ca^{2+} signaling (Haller et al., 1996; Mitchell et al., 2001; Churchill et al., 2002; SantoDomingo et al., 2010), we tested whether acidic organelles play a role in the Ca^{2+} mobilization induced by TRPA1 activation. Bafilomycin A1, a vacuolar-type H^+-ATPase blocker, blocks the acidification of acidic organelles and thus causes Ca^{2+} depletion from these stores (Dröse and Altendorf, 1997; Sankaranarayanan and Ryan, 2001). Interestingly, after pretreatment with bafilomycin A1 (100 nM for 15 min) in the Ca^{2+}-free solution, AITC failed to trigger a $[Ca^{2+}]_i$ increase in DRG neurons (Fig. 3, A and B), whereas the subsequent application of 2.5 mM Ca^{2+} induced a robust $[Ca^{2+}]_i$ rise by the preactivation of TRPA1 channels in the plasma membrane during AITC stimulation (Fig. 3, A and B). Preincubation with 10 μM ruthenium red (RR) blocked the $[Ca^{2+}]_i$ rise through plasma membrane-located TRPA1 (unpublished data). These findings suggest that acidic organelles were essential for the AITC-induced internal Ca^{2+} release. The lysosome is a major acidic organelle. To determine whether lysosomes are critical for the internal Ca^{2+} release evoked by TRPA1 activation, we treated DRG neurons with glycylphenylalanine 2-naphthylamide (GPN; 200 μM for 30 min), a cathepsin C substrate that selectively induces the osmotic lysis of lysosomes (Jadot et al., 1984; Shen et al., 2012). As expected, 200 μM GPN induced a transient $[Ca^{2+}]_i$ rise in DRG neurons bathed in the Ca^{2+}-free solution, and the fluorescent puncta of preloaded Lysotracker Red DND-99 (1 μM; 30 min) diminished after GPN incubation (Fig. 3, C and D). Strikingly, disrupting lysosomes with GPN abolished the AITC-induced $[Ca^{2+}]_i$ rise in DRG neurons in the Ca^{2+}-free solution (control, 53 ± 6 nM; GPN, 1.0 ± 0.7 nM; $P < 0.001$; Fig. 3, E and F), implying that TRPA1 activation induced Ca^{2+} release from lysosome-like organelles. Consistently, GPN pretreatment also substantially reduced the AITC-induced $[Ca^{2+}]_i$ rise in external solution containing the normal Ca^{2+} (2.5 mM), and this was completely blocked by pretreatment with 10 μM RR (Fig. 3, G and H).

To establish the presence of TRPA1 channels in lysosomes, we examined their subcellular localization in DRG neurons by immunofluorescent labeling of TRPA1 and lysosome-

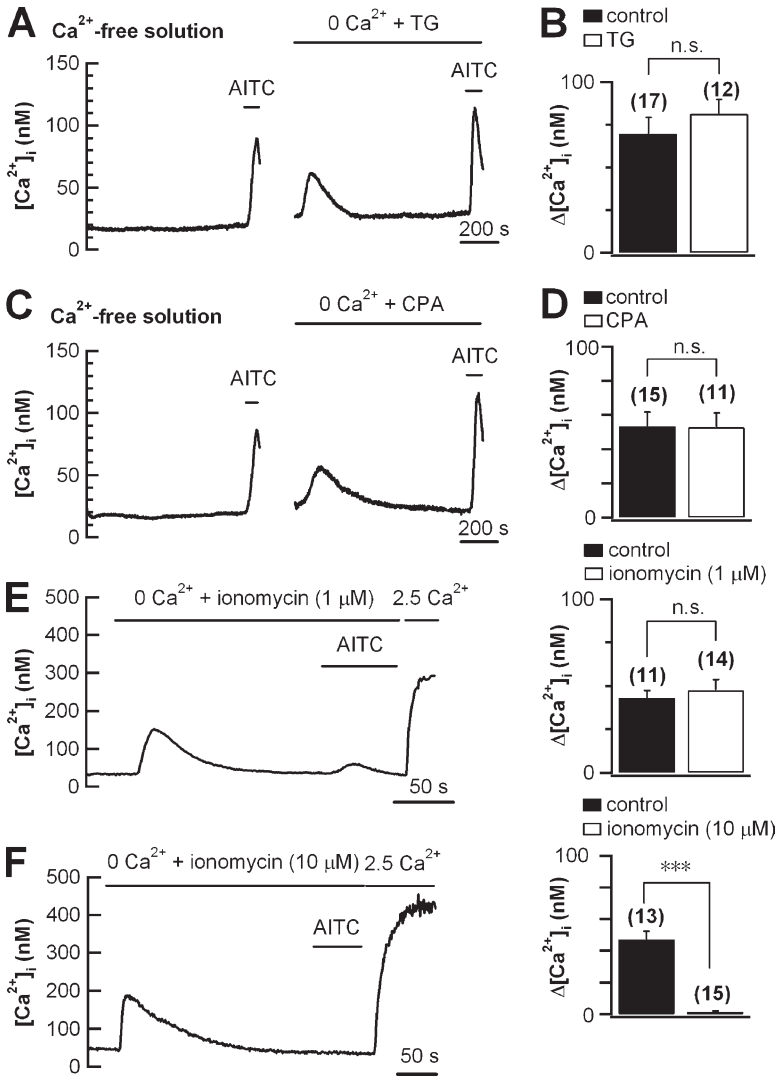

Figure 2. **ER is not involved in Ca^{2+} release induced by TRPA1 channel activation.** (A) Representative traces of AITC-induced Ca^{2+} release in DRG neurons preincubated in Ca^{2+}-free bath solution for 15 min in the absence (left) or presence (right, another cell) of 2.5 µM TG. (B) Statistics of AITC-induced $[Ca^{2+}]_i$ rises as in A. (C and D) Similar to A and B, but 5 µM CPA was used instead of TG. (E and F) AITC-induced $[Ca^{2+}]_i$ changes in DRG neurons pretreated with 1 or 10 µM ionomycin in Ca^{2+}-free bath solution. Ca^{2+} (2.5 mM) was added to the bath immediately after the AITC to show Ca^{2+} influx, which included both TRPA1-mediated Ca^{2+} influx and store-operated Ca^{2+} entry. Quantitative data are on the right. AITC was 100 µM for all experiments. Student's *t* test, ***, $P < 0.001$. Statistical data are presented as mean ± SEM, and *n* values in parentheses represent numbers of cells.

associated membrane protein 1 (LAMP1) or vesicle-associated membrane protein 2 (VAMP2). The specificity of the TRPA1 antibody was confirmed by comparing the labeling of DRG neurons from WT and TRPA1-KO mice. The TRPA1 antibody labeled 26% of the DRG neurons from WT (32 out of 122), but only 2% (4 out of 161) of those (with weak signals) from TRPA1-KO mice (Fig. S4 A). All neurons from WT and TRPA1-KO mice were positively stained by the LAMP1 antibody (Fig. S4 A). Not surprisingly, we found both peripheral and intracellular punctate staining of TRPA1 in WT DRG neurons (Fig. 4 A). Strikingly, TRPA1 mainly colocalized with the lysosome marker LAMP1, especially near the plasma membrane, but was completely separate from the vesicle marker VAMP2 (Fig. 4, A and B; and Fig. S4 B), suggesting the localization of intracellular TRPA1 channels in lysosome-like organelles. Using immunogold labeling and EM, we also detected TRPA1 on the same type of organelles labeled by the LAMP1 antibody (Fig. 4 C). TRPA1 was also found on the plasma membrane, but not in clear vesicles or clathrin-coated pits (Fig. 4 D). Thus, the intracellular Ca^{2+} store targeted by TRPA1 channel activation is most likely associated with lysosomes.

Recently, several groups including ours have directly recorded ionic currents from enlarged endolysosomal vacuoles isolated from cultured fibroblasts, HEK293 cells, and macrophages after treatment with vacuolin-1, a drug that causes endolysosome fusion (Dong et al., 2008; Cang et al., 2013; Feng et al., 2014). We also attempted to isolate vacuoles from vacuolin-treated DRG neurons for whole-endolysosome recording of TRPA1 currents. Unfortunately, we found that although vacuolin-1 generated enlarged vacuoles normally in HEK293 cells, it failed to do so in DRG neurons (Fig. S5), making it impossible to obtain endolysosomal vacuoles suitable for electrophysiological recording. In addition, overexpression of exogenous TRPA1 in HEK293 cells failed to reproduce AITC-induced internal Ca^{2+} release (unpublished data), probably because of their nonneuronal properties or a different protein-modification system in these cells. Thus, endolysosome patch clamp with HEK293 cells could not be used to confirm the functional expression of TRPA1 in lysosomes.

We therefore chose another method to directly monitor AITC-evoked Ca^{2+} release from lysosomes in DRG neurons. We performed confocal line-scan Ca^{2+} imaging with a protocol similar to that of sarcoplasmic reticulum Ca^{2+} sparks (Cheng and Lederer, 2008). The DRG neurons were transfected with LAMP1-EGFP to label endolysosomes (Fig. 5 A). To capture local Ca^{2+} signals, the neurons were loaded with Rhod2 as the Ca^{2+} indicator and EGTA as an intracellular Ca^{2+} buffer. Strikingly, in the Ca^{2+}-free solution, 100 µM AITC induced marked

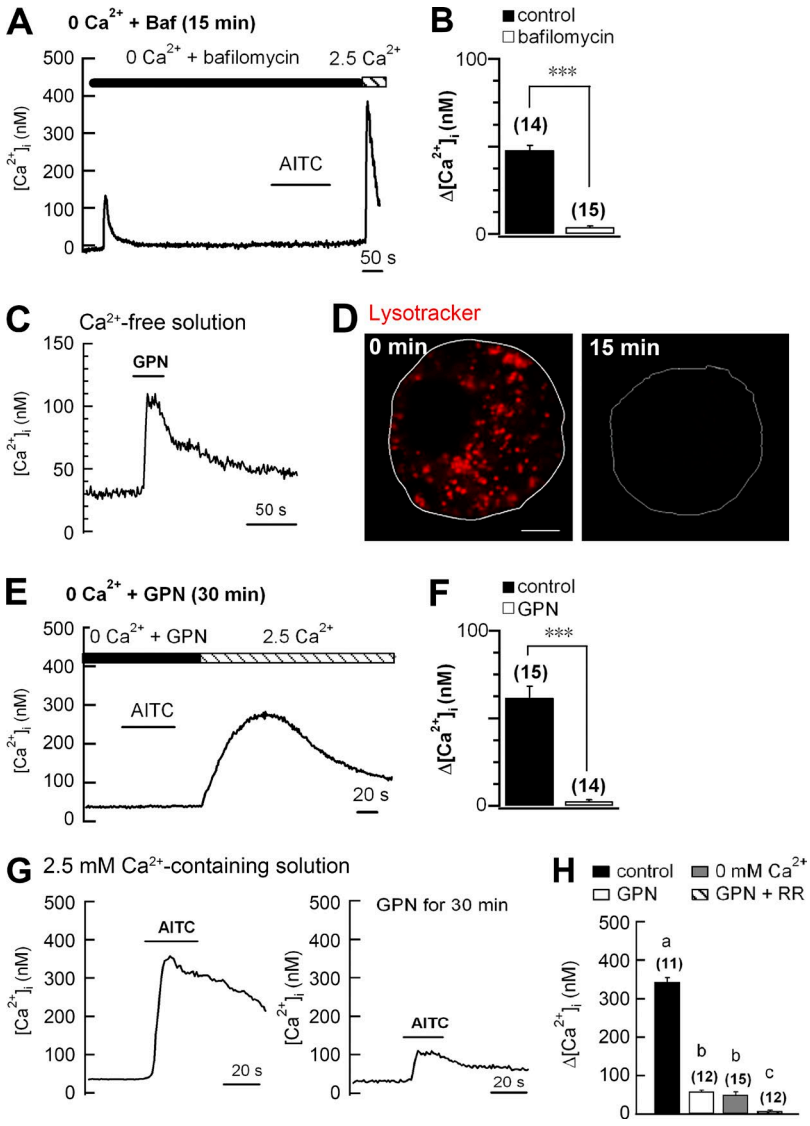

Figure 3. **Disruption of endolysosomal Ca^{2+} storage abolishes the $[Ca^{2+}]_i$ rise in response to TRPA1 channel activation in Ca^{2+}-free bath solution.** (A and B) AITC failed to induce a $[Ca^{2+}]_i$ increase in DRG neurons pretreated with bafilomycin A1 (100 nM, 15 min) in the Ca^{2+}-free bath solution, but subsequent addition of 2.5 mM Ca^{2+} to the bath allowed an immediate $[Ca^{2+}]_i$ increase, showing that TRPA1-mediated Ca^{2+} influx was intact. Quantitative data are shown in B. (C) Representative fluorescence trace showing the transient $[Ca^{2+}]_i$ rise in a DRG neuron in response to 200 µM GPN stimulation in Ca^{2+}-free bath solution. (D) Representative micrographs showing fluorescent puncta of preloaded Lysotracker Red DND-99 (1 µM, 30 min) in a DRG neuron (left) and in another incubated with 200 µM GPN for 15 min (right). Bar, 5 µm. (E and F) AITC failed to induce a $[Ca^{2+}]_i$ increase in DRG neurons pretreated with GPN (200 µM, 30 min) in the Ca^{2+}-free bath solution. Quantitative data are shown in F. (G) Representative fluorescence traces showing that the $[Ca^{2+}]_i$ increase induced by 100 µM AITC in DRG neurons bathed in normal solution containing 2.5 mM Ca^{2+} was markedly reduced by preincubation with 200 µM GPN. (H) Statistics of the AITC-induced $[Ca^{2+}]_i$ rise in DRG neurons and in those pretreated with 200 µM GPN with or without 10 µM RR in normal bath solution. The AITC-induced $[Ca^{2+}]_i$ increase in the Ca^{2+}-free bath solution is included for comparison. Student's *t* test for B and F, one-way ANOVA for H: ***, $P < 0.001$. Values labeled with different letters (a, b, and c) are significantly different from each other. Statistical data are presented as mean ± SEM, and *n* values in parentheses represent numbers of cells.

Ca^{2+} transients in EGFP-labeled regions (lysosome Ca^{2+} sparks), representing Ca^{2+} release from single endolysosomes. In contrast, only minimal Ca^{2+} signals were detected in EGFP-negative regions (Fig. 5, B and C). Consistent with the fact that only a subset of DRG neurons express TRPA1, AITC failed to trigger Ca^{2+} release from individual endolysosomes in ~67% of DRG neurons. These results provided direct evidence that indeed the Ca^{2+} signals arose from lysosome-like organelles upon activation of intracellular TRPA1 channels in DRG neurons.

Ca^{2+} store release contributes to a large and significant fraction of the Ca^{2+} signals generated by TRPA1 channel activation

Previous studies have established that TRPA1 channels mediate Ca^{2+} influx from extracellular space (Karashima et al., 2010). Indeed, a more robust $[Ca^{2+}]_i$ increase was detected in DRG neurons when AITC (100 µM) was applied in the normal Ca^{2+}-containing solution than in the Ca^{2+}-free solution (Fig. 6 A, top traces). To determine whether TRPA1 activation still evoked Ca^{2+} release from the internal store(s) in DRG neurons bathed with normal Ca^{2+}-containing solution, we performed the same experiments but with RR included in the bath. RR is a membrane-impermeable inhibitor that blocks many types of cation channels, including TRPA1 (Story et al., 2003; Hu et al., 2010), and 10 µM RR completely blocks TRPA1 localized on the plasma membrane (Bandell et al., 2004; Jordt et al., 2004). In DRG neurons, pretreatment with 10 µM RR (7 min) significantly reduced, but did not abolish, the $[Ca^{2+}]_i$ rise induced by TRPA1 activation in normal Ca^{2+}-containing solution. The AITC-induced $[Ca^{2+}]_i$ elevation was decreased from 408 ± 26 nM in the absence of RR to 56 ± 10 nM in its presence (Fig. 6, A and D). Consistently, the amplitude of the $[Ca^{2+}]_i$ rise in the presence of RR was similar to that in the Ca^{2+}-free external solution (Fig. 6, A and D).

In addition, pretreatment of DRG neurons with 10 µM RR did not affect the AITC-induced $[Ca^{2+}]_i$ rise in the Ca^{2+}-free external solution (Fig. 6, A and D), consistent with the view that RR is membrane-impermeable and therefore unable to inhibit the $[Ca^{2+}]_i$ rise resulting from internal store release. Collectively, these results showed that activation of TRPA1 channels in normal Ca^{2+}-containing external solution induced a $[Ca^{2+}]_i$ rise through both extracellular Ca^{2+} influx and Ca^{2+} release from internal stores. It seems that RR selectively blocked the Ca^{2+} influx without affecting the Ca^{2+} store release, effectively separating the two processes in the normal Ca^{2+}-containing solution. Given that RR not only blocks Ca^{2+} influx but also inhibits the

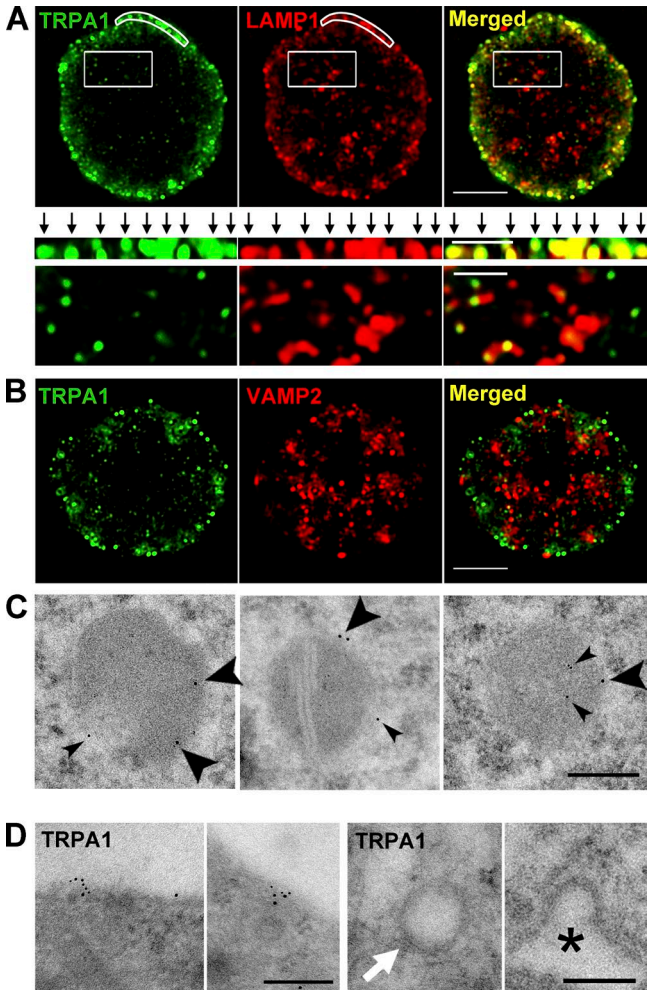

Figure 4. **Localization of intracellular TRPA1 channels to lysosome-like organelles.** (A and B) Representative images captured by an N-SIM superresolution microscope showing immunofluorescent staining for the subcellular localization of TRPA1 in WT DRG neurons. TRPA1-positive staining was prominently colocalized with labeling for the lysosome marker LAMP1 (A) but not that for the vesicle marker VAMP2 (B). For LAMP1, the curved boxes along the plasma membrane were straightened, enlarged, and are shown in the middle panels in A with arrows pointing to colocalized puncta. The rectangular boxes were enlarged and are shown in the bottom panels in A for intracellular puncta. (C) Representative immuno-electron micrographs of subcellular organelles in DRG neurons labeled with antibodies for LAMP1 (10 nm; large arrowheads) and TRPA1 (6 nm; small arrowheads). (D) Representative immuno-electron micrographs of plasma membrane localization of TRPA1 (left two panels). The TRPA1 label was absent from clear vesicles (arrow) and clathrin-coated pits (asterisk; right two panels). Images are representative of three independent cultures. Bars: (A [top] and B) 5 µm; (A, middle and bottom) 2 µm; (C and D) 200 nm.

activity of TRPA1 channels expressed on the plasma membrane, these results further suggested that the Ca^{2+} release induced by TRPA1 activation is independent of not only Ca^{2+} influx from the plasma membrane but also other activities associated with the plasma membrane TRPA1 channels (e.g., Na^+ influx and membrane depolarization).

Activation of TRPA1 channels also triggers membrane depolarization, which may in turn activate voltage-dependent Ca^{2+} channels, an additional means by which Ca^{2+} influx is mediated. Although RR has been shown to block voltage-dependent Ca^{2+} channels in synaptosomes from rat cortex, the affinity appears to be low, with a 50% inhibitory concentration of 70 µM (Hamilton and Lundy, 1995). Consistently, pretreatment (7 min) with 10 µM RR inhibited only 15% of the depolarization-induced $[Ca^{2+}]_i$ rise in DRG neurons (unpublished data), suggesting that the plasma membrane TRPA1 channels were the main target of RR under our experimental conditions.

Because both Ca^{2+} influx and internal Ca^{2+} release contribute to the $[Ca^{2+}]_i$ rise elicited by TRPA1 activation, we next investigated the ratio of the internal store contribution to the overall Ca^{2+} signal in response to TRPA1 activation in DRG neurons in normal Ca^{2+}-containing extracellular medium ($P_{TRPA1\text{-}store}$). We used ΔFd analysis to estimate the percentage of Ca^{2+} arising from internal store release in the total Ca^{2+} rise. ΔFd analysis has been widely used to determine fractional Ca^{2+} currents through TRP and other nonselective cation channels (Schneggenburger et al., 1993; Zeilhofer et al., 1997; Yu et al., 2004; Karashima et al., 2010; also see Materials and methods). When most of the increased Ca^{2+} is bound by Fura-2, ΔFd is an accurate measure of the $[Ca^{2+}]_i$ rise (Zhou and Neher, 1993).

We measured the F_{340} and F_{380} signals and obtained ΔFd by subtracting F_{380} from F_{340} (Yu et al., 2004) for TRPA1-positive DRG neurons stimulated by 100 µM AITC in the presence and absence of extracellular Ca^{2+} (Fig. 6 A, bottom traces). The AITC-induced F_{380} and ΔFd signals from cells bathed in external solution containing either 2.5 or 0 mM Ca^{2+} are shown in Fig. 6 B. From the Fd values, $P_{TRPA1\text{-}store}$ was determined to be ∼40% (ΔFd: 0.25 ± 0.04 arbitrary units [a.u.] in 2.5 mM Ca^{2+} and 0.10 ± 0.01 a.u. in 0 mM Ca^{2+}; Fig. 6, C and E), meaning that internal store release accounts for ∼40% of the overall $[Ca^{2+}]_i$ rise resulting from TRPA1 channel activation in mouse DRG neurons. Supporting this estimate, the AITC-induced $[Ca^{2+}]_i$ rise in GPN-pretreated DRG neurons in the normal Ca^{2+}-containing external solution (contributing extracellular Ca^{2+} influx) was similar to, or slightly larger than, that mediated by store Ca^{2+} release (Fig. 3, G and H).

Ca^{2+} store release induced by TRPA1 channel activation triggers vesicle exocytosis and neuropeptide release from DRG neurons

A rise in $[Ca^{2+}]_i$ directly triggers exocytosis in various cell types (Xu et al., 1998; Yu et al., 2004), so we next investigated whether TRPA1 activation directly triggers exocytosis in DRG neurons. Real-time membrane capacitance (C_m) recordings were used to monitor exocytosis with series conductance (G_s) and membrane conductance (G_m) as controls for seal conditions. AITC evoked a robust C_m increase in WT DRG neurons bathed in the Ca^{2+}-containing solution (Fig. 7 A), suggesting that the AITC-induced $[Ca^{2+}]_i$ rise was sufficient to trigger vesicle exocytosis. In contrast, the AITC-induced C_m increase was drastically decreased in DRG neurons from TRPA1-KO mice (WT, 850 ± 90 fF; TRPA1-KO, 47 ± 1 fF; $P < 0.001$; Fig. 7, E and F). Importantly, AITC also induced exocytosis in WT DRG neurons bathed in the Ca^{2+}-free solution (Fig. 7 B), although the maximal C_m change was 48% smaller than that in normal Ca^{2+}-containing solution (2.5 mM Ca^{2+}, 850 ± 90 fF; 0 mM Ca^{2+}, 450 ± 30 fF; $P < 0.05$; Fig. 7 F). This is consistent with the finding that the AITC-induced $[Ca^{2+}]_i$ increase in the Ca^{2+}-free solution was smaller than that in the Ca^{2+}-containing solution (Fig. 6). To investigate the lysosome dependence of TRPA1 activation-triggered exocytosis in DRG neurons, we dialyzed these cells with 200 µM GPN to induce lysosome osmolysis and found that the AITC-induced C_m increase was

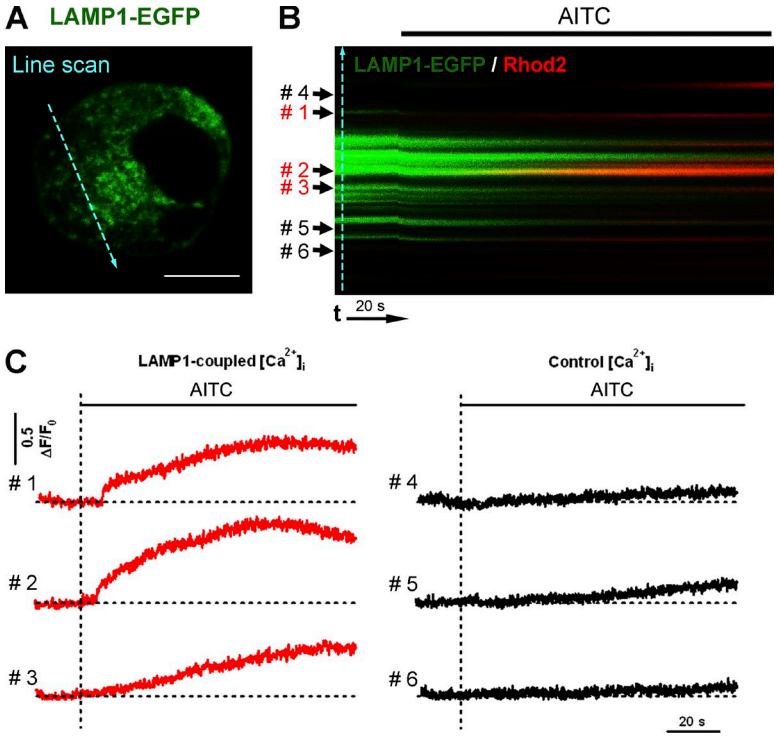

Figure 5. **TRPA1 channel activation induces Ca^{2+} release from individual endolysosomes in mouse DRG neurons.** (A) Representative image of a LAMP1-EGFP–transfected neuron showing the scan-line selection. DRG neurons expressing LAMP1-EGFP were loaded with EGTA-AM and Rhod2-AM and then subjected to confocal line-scan imaging to visualize subcellular compartments involved in AITC-induced Ca^{2+} release. Bar, 10 µm. (B) Line scanning of 100 µM AITC-induced Rhod2 fluorescence over time for the neuron in A. Note the close association of the region showing a Rhod2 fluorescence increase with the EGFP (LAMP1-EGFP) signal. (C) Fluorescence traces of Rhod2 in EGFP-positive (#1–3, lysosome) and EGFP-negative (#4–6, nonlysosome) regions as indicated in B. The results represent 46 lysosome Ca^{2+} release events from nine cells.

markedly reduced 5 min after the dialysis (Fig. 7, C and F) and further decreased when DRG neurons were bathed in the Ca^{2+}-free solution (Fig. 7, D and F). These results demonstrated that TRPA1 activation is coupled to vesicle exocytosis, and TRPA1 channel-mediated Ca^{2+} release from lysosome-like organelles is sufficient to trigger this activity in mouse DRG neurons.

TRP channel activation in peripheral sensory neurons plays essential roles in nociception and pathological pain sensation by causing the release of neuropeptides and other transmitters, such as calcitonin gene-related peptide (CGRP), neuropeptide Y (NPY), and substance P (Ulrich-Lai et al., 2001; Qin et al., 2008; Miyano et al., 2009; Meseguer et al., 2014). To visualize TRPA1 activation-induced neuropeptide release, we transiently expressed NPY-pHluorin in DRG neurons and monitored its release by total internal reflection fluorescence (TIRF) microscopy. Consistent with the idea that TRPA1 activation triggers neuropeptide release, application of AITC induced the exocytosis of large dense-core vesicles labeled with NPY-pHluorin in DRG neurons bathed in both normal and Ca^{2+}-free external solutions (unpublished data). The TIRF imaging experiments thus confirmed the capacitance measurements (Fig. 7, A–E), showing that TRPA1-mediated release of stored Ca^{2+} is sufficient to trigger vesicle release from DRG neurons.

To further confirm that neuropeptide release is evoked by TRPA1 activation, we measured CGRP release from DRG neurons using an enzyme immunometric assay (EIA) kit. In control experiments, increasing the extracellular K^+ concentration from 5 to 100 mM induced a robust CGRP release in 2 mM Ca^{2+}-containing solution (Fig. 8, A and B) under our experimental condition. Application of AITC increased CGRP levels both in the presence and absence of extracellular Ca^{2+} (Fig. 8, C and D), indicating that activation of intracellular TRPA1 alone is sufficient to induce the release of neuropeptides from DRG neurons. In addition, CGRP application substantially enhanced the excitability of DRG neurons (Fig. 8, E and F), implying a role of lysosomal TRPA1 channels in the autoregulation of DRG neurons. To investigate whether lysosomal TRPA1-mediated internal Ca^{2+} release contributes to TRPA1-related pain sensation, we compared lysosomal TRPA1-associated acute noxious sensation between WT and TRPA1 KO mice (Bautista et al., 2006; Kwan et al., 2006; McNamara et al., 2007). Strikingly, topical injection of AITC or acrolein to the rodent hind paws induced the spontaneous nocifensive sensation (flinching and licking) and thermal hyperalgesia (withdrawal latency to thermal noxious stimulation), and they were partially relieved by the preinjection of GPN to deplete the lysosomal Ca^{2+} store (Fig. 9). Altogether, these findings indicate that TRPA1 channels are functionally localized to lysosome-like organelles, and TRPA1-mediated lysosomal Ca^{2+} release plays significant roles in DRG neurons at both the cellular and behavioral levels.

Discussion

Several temperature-sensitive TRP channels (e.g., TRPV1, TRPA1, and TRPM8) are abundantly expressed in DRG neurons and function in temperature sensation and nociception. In this study, we provide the first evidence that, in addition to forming channels on the plasma membrane, TRPA1 is present on lysosomes, and the activation of TRPA1 triggers endolysosomal Ca^{2+} release. Importantly, we demonstrate that the endolysosomal TRPA1 contributes significantly to vesicle exocytosis, neuropeptide/CGRP release, and pain sensation.

The different Ca^{2+} sources and the spatial distribution of Ca^{2+}-permeable channels have important implications for the spatial and temporal patterns of the Ca^{2+} signal, often with specific functional consequences. Conventionally, TRPA1, just like other thermosensitive TRP channels, is thought to work at the plasma membrane and mediate Na^+ and Ca^{2+} influx to elicit nociceptive responses. Although it had been reported that TRPV1 channels may also be present intracellularly and mediate Ca^{2+}

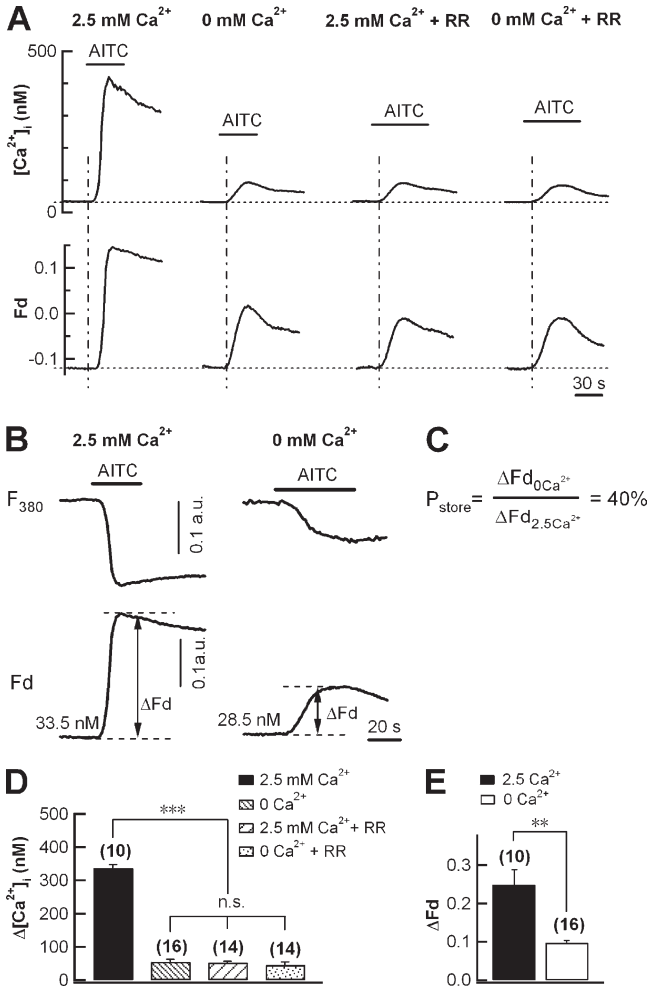

Figure 6. **Comparison of TRPA1 activation-induced Ca^{2+} signals generated by store release versus influx in DRG neurons.** (A) Representative traces of $[Ca^{2+}]_i$ rise (top) and ΔFd (ΔF_{340}-ΔF_{380}; bottom) in DRG neurons induced by 100 µM AITC in 2.5 mM Ca^{2+}-containing or Ca^{2+}-free bath solution in the absence or presence of 10 µM RR. (B–E) Fd analysis of the AITC-induced total $[Ca^{2+}]_i$ rise and that resulting from Ca^{2+} release from internal stores. (B) Representative traces of F_{380} (top) and Fd (bottom) signals induced by TRPA1 activation in bath solution containing 2.5 or 0 mM Ca^{2+}. Basal $[Ca^{2+}]_i$ values are indicated. (C) Equation to estimate P_{store} of TRPA1. (D) Statistics of AITC-induced $[Ca^{2+}]_i$ rises as in A. (E) Statistics of AITC-induced ΔFd signals of DRG neurons bathed in 0 or 2.5 mM Ca^{2+}-containing solution. One-way ANOVA for D, Student's *t* test for E: **, $P < 0.01$; ***, $P < 0.001$. Statistical data are presented as mean ± SEM, and *n* values in parentheses represent numbers of cells.

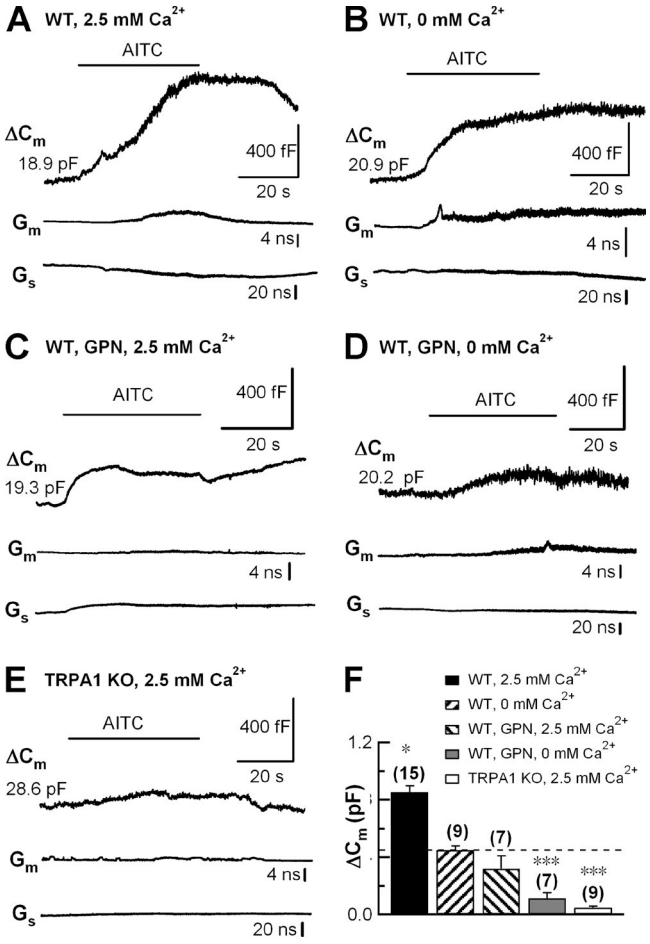

Figure 7. **TRPA1 activation-induced store Ca^{2+} release is sufficient to trigger exocytosis of DRG neurons.** (A and B) Representative C_m traces with the corresponding G_m and G_s showing that 100 µM AITC triggered exocytosis in a DRG neuron bathed in 2.5 mM Ca^{2+}-containing or Ca^{2+}-free external solution. (C and D) Similar to A and B except that the neuron was dialyzed with 200 µM GPN for 5 min under whole-cell conditions before C_m was recorded. (E) Similar to A except that the neuron was from a TRPA1-KO mouse. (F) Statistics of AITC-elicited C_m changes under conditions as in A–E. One-way ANOVA: *, $P < 0.05$; ***, $P < 0.001$. Statistical data are presented as mean ± SEM, and *n* values in parentheses represent numbers of cells.

release, perhaps from the ER (Eun et al., 2001; Gallego-Sandín et al., 2009), the functional implications were not clear. We focused on endogenous TRPA1 channels in native DRG neurons and identified endolysosomes as the compartments from which these channels mediate significant Ca^{2+} release to account for functions previously thought to be mediated only by Ca^{2+} influx through plasma membrane channels. Using ΔFd analysis, we estimated that the lysosomal store release accounted for ∼40% of the overall $[Ca^{2+}]_i$ increase in mouse DRG neurons elicited by 100 µM AITC (Fig. 6). This value is much greater than the contribution of TRPV1-mediated Ca^{2+} release to the overall $[Ca^{2+}]_i$ increase elicited by capsaicin in DRG neurons, which we estimated to be 9% by ΔFd analysis (unpublished data). Therefore, not only do intracellular TRPA1 channels reside in different intracellular compartments from TRPV1 channels, but they may also play a more pronounced role in the apparent cytosolic Ca^{2+} signal than TRPV1 channels.

Membrane proteins are synthesized in the ER and then transported to the plasma membrane. It would, therefore, not be surprising if some ion channels functioned in the ER before being sorted out to the plasma membrane. However, TRPA1 does not appear to act in the ER because predepletion of the ER Ca^{2+} store using TG, CPA, or a low concentration of ionomycin (1 µM) did not affect the intracellular Ca^{2+} release induced by a membrane-permeable TRPA1 agonist (Fig. 2). In contrast, all manipulations that disrupt acidic organelles or lysosomes, such as treatment with bafilomycin A1 and GPN, resulted in the loss of TRPA1 activation-induced intracellular Ca^{2+} release (Fig. 3). Consistent with the pharmacological data, immunostaining and immuno-EM revealed the presence of TRPA1 on both the plasma membrane and lysosome-like organelles in DRG neurons (Fig. 4 and Fig. S4). More importantly, by confocal line-scan imaging of DRG neurons, we demonstrated that AITC-induced Ca^{2+} release occurred in close proximity to

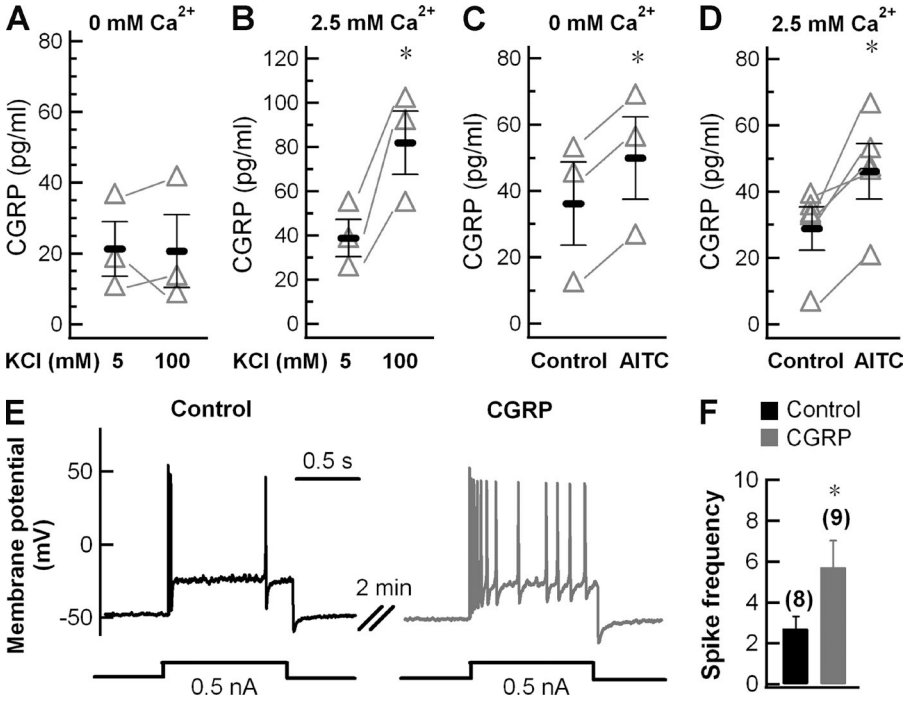

Figure 8. **TRPA1 channel activation mediates CGRP release from DRG neurons in Ca^{2+}-free solution.** (A–D) Mean extracellular CGRP concentrations in the media of primary DRG cultures. Basal CGRP concentrations were measured after 5-min incubation with the normal or Ca^{2+}-free external solution, whereas stimulated CGRP levels were measured after incubation with the same solution containing 100 µM AITC or 100 mM KCl (5 min) as indicated. Different pairs of the assay were conducted with different DRG cultures. At least three independent experiments, each performed in triplicate, are included. (E) Representative action potentials generated by 1-s current injection (500 pA) in a DRG neuron before (Control, left) and during the treatment with 1 µM CGRP (right). (F) Statistics showing the increased spike frequency in DRG neurons in response to CGRP (1 µM) application. Paired Student's *t* test: *, $P < 0.05$. Statistical data are presented as mean ± SEM, and *n* values in parentheses represent numbers of cells.

lysosomes (lysosome Ca^{2+} sparks), whereas the bulk of the cytosol (LAMP1-negative areas) had little response to the TRPA1 agonist under the experimental condition (Fig. 5). Altogether, these data strongly argue for the localization of TRPA1 channels on endolysosomal membranes and their involvement in mediating Ca^{2+} release from these organelles.

Several pieces of evidence suggest that lysosomal TRPA1 channels are critical for TRPA1-mediated physiological functions. First, AITC triggered vesicle exocytosis in Ca^{2+}-free solution (Fig. 7, B and E), suggesting that TRPA1-mediated lysosomal Ca^{2+} release is sufficient to induce exocytosis in DRG neurons. The dramatic inhibition of this response by whole-cell dialysis with 200 µM GPN (Fig. 7, C and E) clearly demonstrated the involvement of lysosomes in the AITC-induced exocytosis under Ca^{2+}-free conditions. Second, TRPA1 activation evoked neuropeptide release from DRG neurons in the absence of extracellular Ca^{2+}. AITC-induced large dense-core vesicle exocytosis was detected by TIRF microscopy imaging (unpublished data) and CGRP release was measured by EIA (Fig. 8, A–D) with samples from DRG neurons bathed in either normal or Ca^{2+}-free external solution. Third, TRPA1-mediated lysosomal Ca^{2+} release plays a significant role in nociception and pain hypersensitivity in mice (Fig. 9). These results further support the idea that TRPA1 activation-induced endolysosomal Ca^{2+} release contributes significantly to vesicle exocytosis and neuropeptide release from DRG neurons and may also contribute to nocifensive sensation.

Collectively, we have shown that TRPA1 activation not only triggers Ca^{2+} influx through the plasma membrane but also elicits Ca^{2+} release from endolysosomes in mouse DRG neurons. TRPA1 activation-induced endolysosomal Ca^{2+} release is of considerable size in the overall Ca^{2+} signal. It directly triggers vesicle exocytosis and neuropeptide release and contributes to nocifensive sensation in mice. These results suggest that multiple Ca^{2+} sources combine to generate distinct Ca^{2+} signatures in DRG neurons in response to the activation of TRPA1 channels and reveal new insights into the physiological and pathological functions of the "multifunctional" TRP channels.

Materials and methods

Cell culture

The use and care of animals were approved and directed by the Animal Care and Use Committee of Peking University. Animals were housed under a 12-h light/dark cycle at 22 ± 2°C (two to four mice per individually ventilated cage) and had free access to food and water. DRG neurons were isolated from adult WT C57BL/6 mice or TRPA1-KO mice of the same strain (20–25 g, male) as previously described (Zhang and Zhou, 2002). The TRPA1-KO mice were provided by D. Julius (University of California, San Francisco, San Francisco, CA). In brief, DRGs were dissected out and placed in ice-cold L15 medium (Gibco). The tissues were then treated with trypsin (0.3 mg/ml) and collagenase (1 mg/ml) for 30 min at 37°C. Cells were dissociated, collected, and plated on coverslips coated with poly-L-lysine (Sigma-Aldrich). They were maintained at 37°C in a 5% CO_2–95% humidified air incubator and used within 2–8 h after plating. For TIRF imaging, the dissociated cells were transfected by electroporation with 3 µg NPY-pHluorin–expressing plasmid using the Neon Transfection System 100 µl kit (MPK10096; Invitrogen) and cultured for 12–18 h in Neurobasal medium (Gibco) supplemented with 2% B27 (Gibco) and GlutaMAX I (Gibco). Except for the unbiased screening of AITC-responsive neurons by Ca^{2+} imaging with confocal microscopy and EIA assays for CGRP release, only small-diameter neurons (20 ± 5 µm, corresponding to type C) were used (Bautista et al., 2006).

Electrophysiological experiments

Patch-clamp recordings were performed using an EPC10/2 amplifier with Pulse software (HEKA). The voltage-clamped whole-cell configuration was used to record C_m and membrane currents in mouse DRG neurons (Zhang and Zhou, 2002). Pipette resistance was between 3 and 4 MΩ, and membrane potential was clamped at ∼70 mV. Normal external solution contained 150 mM NaCl, 5 mM KCl, 2.5 mM $CaCl_2$, 1 mM $MgCl_2$, 10 mM Hepes, and 10 mM glucose, pH 7.4. In the Ca^{2+}-free solution, 2.5 mM $CaCl_2$ was replaced by 1 mM EGTA. Cells were initially bathed in the normal external solution, and then the Ca^{2+}-free solution was locally puffed through a multichannel microperfusion

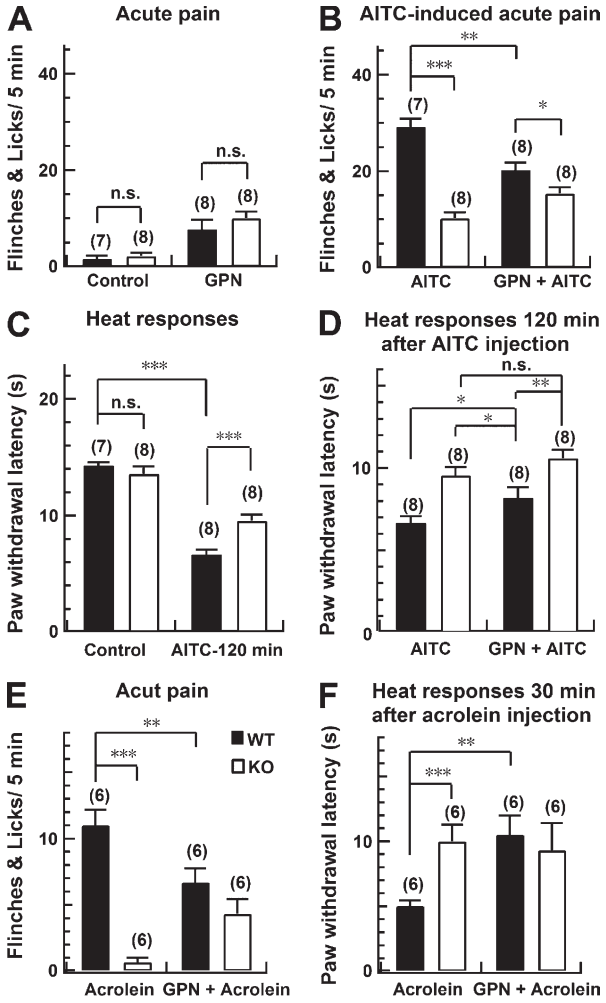

Figure 9. **Lysosomal TRPA1 channels modulate AITC/acrolein-induced spontaneous pain responses and thermal hyperalgesia.** (A) Nocifensive responses (paw flinches and licks) of WT and TRPA1-KO mice measured during 5 min after footpad injection of GPN (20 µl, 2 mM). (B) Nocifensive responses of WT and TRPA1-KO mice measured during 5 min after footpad injection of AITC (20 µl, 100 mM) with or without preinjection of GPN (20 µl, 2 mM). (C and D) Paw withdrawal latency in response to a radiant heat source in WT and TRPA1 KO mice before and 120 min after hind paw injection of AITC (20 µl, 100 mM) with or without preinjection of GPN. (E) Nocifensive responses of WT and TRPA1-KO mice measured as in B, except that acrolein (20 µl, 2 mM) was used instead of AITC. (F) Paw withdrawal latency in response to a radiant heat source in WT and TRPA1 KO mice before and 30 min after footpad injection of acrolein (20 µl, 2 mM) with or without preinjection of GPN. One-way ANOVA: *, $P < 0.05$; **, $P < 0.01$; ***, $P < 0.001$. Statistical data are presented as mean ± SEM, and *n* values in parentheses represent numbers of mice.

system (MPS-2; INBIO). The standard intracellular pipette solution contained 153 mM CsCl, 1 mM $MgCl_2$, 10 mM Hepes, and 4 mM Mg-ATP, pH 7.2. C_m was measured using a lock-in module of the Pulse software as described previously (Zhang and Zhou, 2002). In brief, a 1-kHz, 20-mV peak-to-peak sinusoid was applied around a holding potential of −70 mV. Currents were recorded with the Pulse software at a sampling rate of 5 kHz. Drugs were delivered using the MPS-2 system as stated in this section above. Data were analyzed using the Lindau-Neher technique to estimate C_m, G_m, and G_s. Only recordings without significant changes of G_m and G_s were used for analysis (Zhang and Zhou, 2002).

Intracellular Ca^{2+} measurement

Photometric measurement of $[Ca^{2+}]_i$ was performed as previously reported (Zhang and Zhou, 2002; Yu et al., 2004). In brief, DRG neurons were loaded with 5 µM Fura-2 AM (Invitrogen) for 5 min at 37°C. Cells were then washed three times (1 min each) with normal external solution at room temperature. An IX-70 inverted microscope (Olympus) equipped with a monochromator-based system (TILL Photonics) was used to monitor fluorescence changes with alternating excitation wavelengths of 340 and 380 nm. Emitted light at 510 nm was acquired through a photomultiplier tube (TILL Photonics) and recorded by the Pulse software. The fluorescence was sampled at 2 Hz (Zhang and Zhou, 2002). $[Ca^{2+}]_i$ was calculated from the ratio (R) of the fluorescence signals excited at 340 nm and 380 nm with the following equation: $[Ca^{2+}]_i = K_d \times (R - R_{min})/(R_{max} - R)$. K_d, R_{min}, and R_{max} are constants obtained from in vitro calibration as previously described (Xu et al., 1998). To avoid the desensitization of TRPA1 channels by drug application, only one cell per coverslip was used for AITC-induced signals. To block TRPA1 channels located on the plasma membrane, DRG neurons were incubated with 10 µM RR for 7 min at room temperature before the ratiometric $[Ca^{2+}]_i$ measurement.

For unbiased screening of TRPA1-positive cells, DRG neurons from WT and TRPA1 KO mice were loaded with 5 µM Fluo4-AM and imaged on an inverted confocal microscope (LSM710; ZEISS). Fluorescence images were captured by excitation with a 488-nm laser and emission at 500–560 nm. AITC (100 µM) or KCl (70 mM) was applied locally to the cells by a gravity-fed perfusion system. Fluorescence intensity values from the images were calculated and analyzed using ImageJ (National Institutes of Health). Images were acquired for >20 s before stimulation to establish a stable baseline, and then the fluorescence intensity values during the first 10 s before stimulation were averaged and used for normalization. Neurons that showed fluorescence changes (ΔF) >0.5 in response to stimulation were defined as AITC/4-HNE–responsive cells. This cutoff for selection (5 a.u.) is 1.5-fold that of the full-width half maximum of the Gaussian distribution of fluorescence noise.

For confocal line-scan imaging, mouse DRG neurons were transfected with LAMP1-EGFP and cultured for 12–18 h before experiments. Transfected neurons were incubated with 5 µM EGTA-AM (Invitrogen) for 15 min followed by 5 µM Rhod2-AM (Invitrogen) for 5 min. Cells were washed with standard bath solution immediately after incubation. A z-series of 1-µm optical sections was imaged using a 710 inverted confocal microscope with a 40× oil immersion lens (ZEISS). Line-scan mode was used to measure local Ca^{2+} signals. DRG neurons were bathed in the standard bath solution. The Ca^{2+}-free bath solution was locally delivered to the cell by a drug-puffing device (MPS1; Shanghai Yibo Instruments Co., Ltd.) for 60 s before and during the first 20 s of line-scan imaging. The puffing solution was changed to 100 µM AITC in the Ca^{2+}-free solution to trigger intracellular Ca^{2+} release during line-scanning. Fluorescence intensities of Rhod2 and GFP (for LAMP1-EGFP) along the line were recorded alternately by excitation at 543 and 488 nm and emission at 560–620 and 500–535 nm at 100 Hz. Changes in Rhod2 fluorescence intensity in EGFP-positive (lysosome) and EGFP-negative (nonlysosome control) regions over time were calculated using the plot profile function of ImageJ and plotted as $\Delta F/F_0$ against time to indicate local $[Ca^{2+}]_i$ changes.

Immunofluorescence and N-SIM superresolution imaging

DRG neurons were fixed with 4% PFA in PBS for 20 min and permeabilized with 0.3% Triton X-100 (in PBS with 2% BSA) for 5 min. Cells were then blocked with 2% BSA in PBS for 1 h. Primary

antibodies were diluted in PBS with 2% BSA and incubated overnight at 4°C. After washing out the primary antibodies with the blocking solution, cells were incubated for 1 h with Alexa Fluor 488– or 594–conjugated secondary antibodies (A11029, A11037, and A11055; Invitrogen). Antibodies against TRPA1 (ANKTM1 [F-20]; sc-32355; Santa Cruz Biotechnology, Inc.), VAMP2 (104211; Synaptic Systems), and LAMP1 (ab25744; Abcam) were used. Images were captured using an N-SIM superresolution microscope system with 78-nm resolution in the x and y axes and 300 nm in the z axis (Nikon). Images were processed using ImageJ.

Immunogold labeling and EM

Tissue slices of lumbar (L4–L6) DRGs were fixed in 2.5% glutaraldehyde and 2% PFA in PBS for 3 h at room temperature. After washing with PBS, they were dehydrated through an ethanol series, embedded in LR white resin, polymerized at 50°C for 24 h, and sectioned at 80 nm. The sections were collected on single-slot, formvar-coated nickel grids. After blocking in 5% BSA in PBS, they were incubated with antibodies against TRPA1 (Santa Cruz Biotechnology, Inc.) and/or LAMP1 (Abcam), washed, and incubated with secondary antibodies (LAMP1: goat anti–rabbit IgG conjugated to 10-nm gold particles, G7277 [Invitrogen]; TRPA1: donkey anti–goat IgG conjugated to 6-nm gold particles, 806.333 [AURION]; or rabbit anti–goat IgG conjugated to 10-nm gold particles, G5402 [Sigma-Aldrich]). Tissue sections were poststained with 2% uranyl acetate for 8–10 min and imaged under a transmission electron microscope (Tecnai G2 20; 200 kV; Thermo Fisher Scientific).

Fractional contribution of Ca^{2+} store

The fractional contribution of the Ca^{2+} store (P_{store}) was defined as the percentage of Ca^{2+} arising from internal store release in the total $[Ca^{2+}]_i$ rise through TRP channels localized both on the plasma membrane and the internal store (Neher and Augustine, 1992; Schneggenburger et al., 1993; Zhou and Neher, 1993; Yu et al., 2004). To control the intracellular Fura-2 concentration ($[Fura\text{-}2]_i$), we kept loading conditions uniform for all DRG neurons and only imaged those that had about the same diameter (20 ± 2 µm). For P_{store} measurement, Fura-2 AM stock solution was freshly made each time and used at 5 µM. A standard F_{360}-$[Fura\text{-}2]_i$ plot was generated by loading known concentrations of Fura-2 potassium salt into rat DRG neurons using the whole-cell configuration of the patch clamp method and measuring the corresponding F_{360} signal ([Fura-2] [mM]/F_{360} [a.u.]: 0.125/0.543, 0.25/0.764, 0.5/1.818, and 1/3.038). The $F_{360} - [Fura\text{-}2]_i$ relationship was determined to be $F_{360} = 2.93 \times [Fura\text{-}2]_i + 0.17$ ($R^2 = 0.99$; Zhou and Neher, 1993). The mean F_{360} value of small Fura-2 AM–loaded DRG neurons was 0.52 ± 0.02, thus giving an estimated $[Fura\text{-}2]_i$ in the loaded mouse neurons of 120 µM. Because higher $[Fura\text{-}2]_i$ reduced the basal $[Ca^{2+}]_i$, which is needed for TRPA1 activation (Bautista et al., 2006; Zurborg et al., 2007), we determined the fractional contribution of Ca^{2+} store release against the total Ca^{2+} signal (release plus influx) under conditions in which intracellular Ca^{2+} buffers were similar at both 0 and 2.5 mM extracellular Ca^{2+}. In this way, a similar fraction of Ca^{2+} release and Ca^{2+} influx (termed Pf) would be captured by nonsaturating Fura-2 in the same cell. Assuming the same Pf value for Q_{store} and Q_{total}, we have $P_{store} = Q_{TRP\text{-}store}/Q_{TRP\text{-}total} = (\Delta Fd_{0Ca}/Pf)/(\Delta Fd_{2.5Ca}/Pf) = \Delta Fd_{0Ca}/\Delta Fd_{2.5Ca}$, in which ΔFd_{0Ca} and $\Delta Fd_{2.5Ca}$ are ΔFd values at 0 and 2.5 mM extracellular Ca^{2+}.

CGRP immunoassay

Basal and stimulated extracellular CGRP concentrations were evaluated in freshly isolated DRG neurons using an EIA kit (Bachem) following the manufacturer's instructions. The isolated cells were maintained in DMEM/F12 with 10% FBS for 2–3 h in a 24-well plate before EIA experiments. For each well, cells were washed three times with normal external solution and then incubated with normal or Ca^{2+}-free external solution for 5 min at room temperature, followed by another 5-min incubation with the same solution containing 100 µM AITC. The incubating solutions were collected for subsequent analysis of basal and stimulation-coupled CGRP levels. A similar protocol was used for 100 mM K^+-induced CGRP release from DRG neurons in normal external solution. All samples were centrifuged at 13,000 rpm for 5 min and the supernatants processed for CGRP measurement. Samples were analyzed at 450 nm with a microplate reader (Synergy 4; BioTek). CGRP concentrations (in picograms per milliliter) were extrapolated from a best-fit line calculated from serial dilutions of a CGRP standard. All data points were measured in triplicate.

Behavioral studies

Mice were housed under a 12-h light/dark cycle at 22 ± 2°C, and experiments were performed in the afternoon. Flinching and licking responses to AITC/acrolein were monitored and quantified following previously described methods (Bautista et al., 2006; Kwan et al., 2006). AITC (20 µl, 100 mM) or acrolein (20 µl, 2 mM) was injected into the right hind footpad. Pain was assessed by paw flinching and licking during 5 min after injection. To investigate the effect of GPN on AITC/acrolein-induced spontaneous nocifensive sensation and thermal hyperalgesia, GPN (20 µl, 2 mM) was injected 15 min before the injection of AITC/acrolein plus GPN (20 µl, same concentrations as listed previously). In the thermal nociception assay, mice were allowed to acclimate to a Plexiglas chamber for at least 30 min every day for 1 wk before experiments. The plantar test (3730-002; Ugo Basile) was used to assess thermal hyperalgesia; mice were placed on the surface of a 2-mm–thick glass plate, and a radiant heat stimulus was applied under the glass floor according to literature (Caterina et al., 2000; Bautista et al., 2006). The heat stimulus was terminated with a withdrawal response or a cutoff value of 20 s to prevent injury. The paw withdrawal latency was defined as the time from the beginning of the heat stimulus to hind paw withdrawal. To assess AITC/acrolein-induced thermal hyperalgesia, 20 µl AITC (100 mM) or acrolein (2 mM) was injected into the right hind footpad with or without preinjection of 2 mM GPN 120 (for AITC) or 30 min (for acrolein) before the thermal nociception test. The experimenters were blinded to the genotypes of the mice for all of the behavioral experiments.

Drugs and reagents

All chemicals were from Sigma-Aldrich unless otherwise specified.

Statistics

All experiments were replicated at least three times. All electrophysiological data were analyzed with Igor software. Statistical comparisons were performed with the two-tailed unpaired Student's *t* test or one-way analysis of variance (ANOVA) as indicated using Statistical Package for the Social Sciences 13.0. No statistical methods were used to predetermine sample sizes, but our sample sizes are similar to those generally used in the field. Normality of the data were tested with the Shapiro-Wilk test, and the equality of variance was determined with Lenene's test. Statistical data are presented as mean ± SEM, and a significant difference was accepted at $P < 0.05$. Numbers of cells or animals analyzed are indicated in the figures.

Online supplemental material

Fig. S1 shows that AITC induces a $[Ca^{2+}]_i$ rise in DRG neurons bathed in normal Ca^{2+}-containing solution and that 4-HNE induces a $[Ca^{2+}]_i$ rise in DRG neurons bathed in Ca^{2+}-free solution. Fig. S2 shows that TRPA1 activation mediates $[Ca^{2+}]_i$ rise in DRG neurons bathed in

normal Ca^{2+}-containing solution. Fig. S3 shows that TRPA1 activation mediates a $[Ca^{2+}]_i$ rise in DRG neurons bathed in Ca^{2+}-free solution. Fig. S4 shows the localization of TRPA1 channels in endolysosomes in DRG neurons. Fig. S5 shows that vacuolin-1 fails to enlarge endolysosomes in DRG neurons.

Acknowledgments

The authors thank Dr. Heping Peace Cheng (Institute of Molecular Medicine, Peking University) for advice on the confocal line-scan imaging of lysosome Ca^{2+} sparks, Dr. Yingchun Hu (Core Facilities, College of Life Sciences, Peking University) for assistance with the transmission EM experiments, and Dr. Iain C. Bruce (Institute of Molecular Medicine, Peking University) for helpful comments on the manuscript.

This work was supported by grants from the National Basic Research Program of China (2012CB518006) and the National Natural Science Foundation of China (31228010, 31171026, 31100597, 31327901, 31221002, 31330024, 31400708, 31670843, 31521062, and SQ2011SF11B01041). M.X. Zhu was supported by the National Institutes of Health (grants R01DK081654 and R01GM081658). C. Wang was supported in part by a Postdoctoral Fellowship from the Peking-Tsinghua Center for Life Sciences.

The authors declare no competing financial interests.

Submitted: 24 March 2016
Revised: 16 August 2016
Accepted: 4 October 2016

References

Akude, E., E. Zherebitskaya, S.K. Roy Chowdhury, K. Girling, and P. Fernyhough. 2010. 4-Hydroxy-2-nonenal induces mitochondrial dysfunction and aberrant axonal outgrowth in adult sensory neurons that mimics features of diabetic neuropathy. *Neurotox. Res.* 17:28–38. http://dx.doi.org/10.1007/s12640-009-9074-5

Andersson, D.A., C. Gentry, S. Moss, and S. Bevan. 2008. Transient receptor potential A1 is a sensory receptor for multiple products of oxidative stress. *J. Neurosci.* 28:2485–2494. http://dx.doi.org/10.1523/JNEUROSCI.5369-07.2008

Bandell, M., G.M. Story, S.W. Hwang, V. Viswanath, S.R. Eid, M.J. Petrus, T.J. Earley, and A. Patapoutian. 2004. Noxious cold ion channel TRPA1 is activated by pungent compounds and bradykinin. *Neuron.* 41:849–857. http://dx.doi.org/10.1016/S0896-6273(04)00150-3

Bautista, D.M., S.E. Jordt, T. Nikai, P.R. Tsuruda, A.J. Read, J. Poblete, E.N. Yamoah, A.I. Basbaum, and D. Julius. 2006. TRPA1 mediates the inflammatory actions of environmental irritants and proalgesic agents. *Cell.* 124:1269–1282. http://dx.doi.org/10.1016/j.cell.2006.02.023

Berridge, M.J. 2005. Unlocking the secrets of cell signaling. *Annu. Rev. Physiol.* 67:1–21. http://dx.doi.org/10.1146/annurev.physiol.67.040103.152647

Brocard, J.B., M. Tassetto, and I.J. Reynolds. 2001. Quantitative evaluation of mitochondrial calcium content in rat cortical neurones following a glutamate stimulus. *J. Physiol.* 531:793–805. http://dx.doi.org/10.1111/j.1469-7793.2001.0793h.x

Cang, C., Y. Zhou, B. Navarro, Y.J. Seo, K. Aranda, L. Shi, S. Battaglia-Hsu, I. Nissim, D.E. Clapham, and D. Ren. 2013. mTOR regulates lysosomal ATP-sensitive two-pore Na^+ channels to adapt to metabolic state. *Cell.* 152:778–790. http://dx.doi.org/10.1016/j.cell.2013.01.023

Caterina, M.J., A. Leffler, A.B. Malmberg, W.J. Martin, J. Trafton, K.R. Petersen-Zeitz, M. Koltzenburg, A.I. Basbaum, and D. Julius. 2000. Impaired nociception and pain sensation in mice lacking the capsaicin receptor. *Science.* 288:306–313. http://dx.doi.org/10.1126/science.288.5464.306

Cheng, H., and W.J. Lederer. 2008. Calcium sparks. *Physiol. Rev.* 88:1491–1545. http://dx.doi.org/10.1152/physrev.00030.2007

Churchill, G.C., Y. Okada, J.M. Thomas, A.A. Genazzani, S. Patel, and A. Galione. 2002. NAADP mobilizes Ca(2+) from reserve granules, lysosome-related organelles, in sea urchin eggs. *Cell.* 111:703–708. http://dx.doi.org/10.1016/S0092-8674(02)01082-6

Dong, X.P., X. Cheng, E. Mills, M. Delling, F. Wang, T. Kurz, and H. Xu. 2008. The type IV mucolipidosis-associated protein TRPML1 is an endolysosomal iron release channel. *Nature.* 455:992–996. http://dx.doi.org/10.1038/nature07311

Dröse, S., and K. Altendorf. 1997. Bafilomycins and concanamycins as inhibitors of V-ATPases and P-ATPases. *J. Exp. Biol.* 200:1–8.

Due, M.R., J. Park, L. Zheng, M. Walls, Y.M. Allette, F.A. White, and R. Shi. 2014. Acrolein involvement in sensory and behavioral hypersensitivity following spinal cord injury in the rat. *J. Neurochem.* 128:776–786. http://dx.doi.org/10.1111/jnc.12500

Emptage, N.J., C.A. Reid, and A. Fine. 2001. Calcium stores in hippocampal synaptic boutons mediate short-term plasticity, store-operated Ca^{2+} entry, and spontaneous transmitter release. *Neuron.* 29:197–208. http://dx.doi.org/10.1016/S0896-6273(01)00190-8

Eun, S.Y., S.J. Jung, Y.K. Park, J. Kwak, S.J. Kim, and J. Kim. 2001. Effects of capsaicin on Ca^{2+} release from the intracellular Ca^{2+} stores in the dorsal root ganglion cells of adult rats. *Biochem. Biophys. Res. Commun.* 285:1114–1120. http://dx.doi.org/10.1006/bbrc.2001.5272

Everaerts, W., M. Gees, Y.A. Alpizar, R. Farre, C. Leten, A. Apetrei, I. Dewachter, F. van Leuven, R. Vennekens, D. De Ridder, et al. 2011. The capsaicin receptor TRPV1 is a crucial mediator of the noxious effects of mustard oil. *Curr. Biol.* 21:316–321. http://dx.doi.org/10.1016/j.cub.2011.01.031

Feng, X., Y. Huang, Y. Lu, J. Xiong, C.O. Wong, P. Yang, J. Xia, D. Chen, G. Du, K. Venkatachalam, et al. 2014. *Drosophila* TRPML forms PI(3,5)P2-activated cation channels in both endolysosomes and plasma membrane. *J. Biol. Chem.* 289:4262–4272. http://dx.doi.org/10.1074/jbc.M113.506501

Foyouzi-Youssefi, R., S. Arnaudeau, C. Borner, W.L. Kelley, J. Tschopp, D.P. Lew, N. Demaurex, and K.H. Krause. 2000. Bcl-2 decreases the free Ca^{2+} concentration within the endoplasmic reticulum. *Proc. Natl. Acad. Sci. USA.* 97:5723–5728. http://dx.doi.org/10.1073/pnas.97.11.5723

Gallego-Sandín, S., A. Rodríguez-García, M.T. Alonso, and J. García-Sancho. 2009. The endoplasmic reticulum of dorsal root ganglion neurons contains functional TRPV1 channels. *J. Biol. Chem.* 284:32591–32601. http://dx.doi.org/10.1074/jbc.M109.019687

Grienberger, C., and A. Konnerth. 2012. Imaging calcium in neurons. *Neuron.* 73:862–885. http://dx.doi.org/10.1016/j.neuron.2012.02.011

Haller, T., P. Dietl, P. Deetjen, and H. Völkl. 1996. The lysosomal compartment as intracellular calcium store in MDCK cells: A possible involvement in InsP3-mediated Ca^{2+} release. *Cell Calcium.* 19:157–165. http://dx.doi.org/10.1016/S0143-4160(96)90084-6

Hamilton, M.G., and P.M. Lundy. 1995. Effect of ruthenium red on voltage-sensitive Ca^{++} channels. *J. Pharmacol. Exp. Ther.* 273:940–947.

Hu, H., J. Tian, Y. Zhu, C. Wang, R. Xiao, J.M. Herz, J.D. Wood, and M.X. Zhu. 2010. Activation of TRPA1 channels by fenamate nonsteroidal anti-inflammatory drugs. *Pflugers Arch.* 459:579–592. http://dx.doi.org/10.1007/s00424-009-0749-9

Jadot, M., C. Colmant, S. Wattiaux-De Coninck, and R. Wattiaux. 1984. Intralysosomal hydrolysis of glycyl-L-phenylalanine 2-naphthylamide. *Biochem. J.* 219:965–970. http://dx.doi.org/10.1042/bj2190965

Jordt, S.E., D.M. Bautista, H.H. Chuang, D.D. McKemy, P.M. Zygmunt, E.D. Högestätt, I.D. Meng, and D. Julius. 2004. Mustard oils and cannabinoids excite sensory nerve fibres through the TRP channel ANKTM1. *Nature.* 427:260–265. http://dx.doi.org/10.1038/nature02282

Karashima, Y., K. Talavera, W. Everaerts, A. Janssens, K.Y. Kwan, R. Vennekens, B. Nilius, and T. Voets. 2009. TRPA1 acts as a cold sensor in vitro and in vivo. *Proc. Natl. Acad. Sci. USA.* 106:1273–1278. http://dx.doi.org/10.1073/pnas.0808487106

Karashima, Y., J. Prenen, K. Talavera, A. Janssens, T. Voets, and B. Nilius. 2010. Agonist-induced changes in Ca^{2+} permeation through the nociceptor cation channel TRPA1. *Biophys. J.* 98:773–783. http://dx.doi.org/10.1016/j.bpj.2009.11.007

Kwan, K.Y., A.J. Allchorne, M.A. Vollrath, A.P. Christensen, D.S. Zhang, C.J. Woolf, and D.P. Corey. 2006. TRPA1 contributes to cold, mechanical, and chemical nociception but is not essential for hair-cell transduction. *Neuron.* 50:277–289. http://dx.doi.org/10.1016/j.neuron.2006.03.042

Lupachyk, S., H. Shevalye, Y. Maksimchyk, V.R. Drel, and I.G. Obrosova. 2011. PARP inhibition alleviates diabetes-induced systemic oxidative stress and neural tissue 4-hydroxynonenal adduct accumulation: Correlation with peripheral nerve function. *Free Radic. Biol. Med.* 50:1400–1409. http://dx.doi.org/10.1016/j.freeradbiomed.2011.01.037

Macpherson, L.J., B. Xiao, K.Y. Kwan, M.J. Petrus, A.E. Dubin, S. Hwang, B. Cravatt, D.P. Corey, and A. Patapoutian. 2007. An ion channel essential for sensing chemical damage. *J. Neurosci.* 27:11412–11415. http://dx.doi.org/10.1523/JNEUROSCI.3600-07.2007

McNamara, C.R., J. Mandel-Brehm, D.M. Bautista, J. Siemens, K.L. Deranian, M. Zhao, N.J. Hayward, J.A. Chong, D. Julius, M.M. Moran, and C.M. Fanger. 2007. TRPA1 mediates formalin-induced pain. *Proc. Natl. Acad. Sci. USA.* 104:13525–13530. http://dx.doi.org/10.1073/pnas.0705924104

Meseguer, V., Y.A. Alpizar, E. Luis, S. Tajada, B. Denlinger, O. Fajardo, J.A. Manenschijn, C. Fernández-Peña, A. Talavera, T. Kichko, et al. 2014. TRPA1 channels mediate acute neurogenic inflammation and pain produced by bacterial endotoxins. *Nat. Commun.* 5:3125. http://dx.doi.org/10.1038/ncomms4125

Mitchell, K.J., P. Pinton, A. Varadi, C. Tacchetti, E.K. Ainscow, T. Pozzan, R. Rizzuto, and G.A. Rutter. 2001. Dense core secretory vesicles revealed as a dynamic Ca^{2+} store in neuroendocrine cells with a vesicle-associated membrane protein aequorin chimaera. *J. Cell Biol.* 155:41–51. http://dx.doi.org/10.1083/jcb.200103145

Miyano, K., H.B. Tang, Y. Nakamura, N. Morioka, A. Inoue, and Y. Nakata. 2009. Paclitaxel and vinorelbine, evoked the release of substance P from cultured rat dorsal root ganglion cells through different PKC isoform-sensitive ion channels. *Neuropharmacology.* 57:25–32. http://dx.doi.org/10.1016/j.neuropharm.2009.04.001

Montell, C. 2011. The history of TRP channels, a commentary and reflection. *Pflugers Arch.* 461:499–506. http://dx.doi.org/10.1007/s00424-010-0920-3

Neher, E., and G.J. Augustine. 1992. Calcium gradients and buffers in bovine chromaffin cells. *J. Physiol.* 450:273–301. http://dx.doi.org/10.1113/jphysiol.1992.sp019127

Qin, N., M.P. Neeper, Y. Liu, T.L. Hutchinson, M.L. Lubin, and C.M. Flores. 2008. TRPV2 is activated by cannabidiol and mediates CGRP release in cultured rat dorsal root ganglion neurons. *J. Neurosci.* 28:6231–6238. http://dx.doi.org/10.1523/JNEUROSCI.0504-08.2008

Ruparel, N.B., A.M. Patwardhan, A.N. Akopian, and K.M. Hargreaves. 2008. Homologous and heterologous desensitization of capsaicin and mustard oil responses utilize different cellular pathways in nociceptors. *Pain.* 135:271–279. http://dx.doi.org/10.1016/j.pain.2007.06.005

Sankaranarayanan, S., and T.A. Ryan. 2001. Calcium accelerates endocytosis of vSNAREs at hippocampal synapses. *Nat. Neurosci.* 4:129–136. http://dx.doi.org/10.1038/83949

SantoDomingo, J., R.I. Fonteriz, C.D. Lobatón, M. Montero, A. Moreno, and J. Alvarez. 2010. Ca2+ dynamics in the secretory vesicles of neurosecretory PC12 and INS1 cells. *Cell. Mol. Neurobiol.* 30:1267–1274. http://dx.doi.org/10.1007/s10571-010-9572-2

Schmidt, M., A.E. Dubin, M.J. Petrus, T.J. Earley, and A. Patapoutian. 2009. Nociceptive signals induce trafficking of TRPA1 to the plasma membrane. *Neuron.* 64:498–509. http://dx.doi.org/10.1016/j.neuron.2009.09.030

Schneggenburger, R., Z. Zhou, A. Konnerth, and E. Neher. 1993. Fractional contribution of calcium to the cation current through glutamate receptor channels. *Neuron.* 11:133–143. http://dx.doi.org/10.1016/0896-6273(93)90277-X

Seidler, N.W., I. Jona, M. Vegh, and A. Martonosi. 1989. Cyclopiazonic acid is a specific inhibitor of the Ca^{2+}-ATPase of sarcoplasmic reticulum. *J. Biol. Chem.* 264:17816–17823.

Shen, D., X. Wang, X. Li, X. Zhang, Z. Yao, S. Dibble, X.P. Dong, T. Yu, A.P. Lieberman, H.D. Showalter, and H. Xu. 2012. Lipid storage disorders block lysosomal trafficking by inhibiting a TRP channel and lysosomal calcium release. *Nat. Commun.* 3:731. http://dx.doi.org/10.1038/ncomms1735

Story, G.M., A.M. Peier, A.J. Reeve, S.R. Eid, J. Mosbacher, T.R. Hricik, T.J. Earley, A.C. Hergarden, D.A. Andersson, S.W. Hwang, et al. 2003. ANKTM1, a TRP-like channel expressed in nociceptive neurons, is activated by cold temperatures. *Cell.* 112:819–829. http://dx.doi.org/10.1016/S0092-8674(03)00158-2

Trevisani, M., J. Siemens, S. Materazzi, D.M. Bautista, R. Nassini, B. Campi, N. Imamachi, E. Andrè, R. Patacchini, G.S. Cottrell, et al. 2007. 4-Hydroxynonenal, an endogenous aldehyde, causes pain and neurogenic inflammation through activation of the irritant receptor TRPA1. *Proc. Natl. Acad. Sci. USA.* 104:13519–13524. http://dx.doi.org/10.1073/pnas.0705923104

Ulrich-Lai, Y.M., C.M. Flores, C.A. Harding-Rose, H.E. Goodis, and K.M. Hargreaves. 2001. Capsaicin-evoked release of immunoreactive calcitonin gene-related peptide from rat trigeminal ganglion: Evidence for intraganglionic neurotransmission. *Pain.* 91:219–226. http://dx.doi.org/10.1016/S0304-3959(00)00439-5

Wu, L.J., T.B. Sweet, and D.E. Clapham. 2010. International Union of Basic and Clinical Pharmacology. LXXVI. Current progress in the mammalian TRP ion channel family. *Pharmacol. Rev.* 62:381–404. http://dx.doi.org/10.1124/pr.110.002725

Xu, T., T. Binz, H. Niemann, and E. Neher. 1998. Multiple kinetic components of exocytosis distinguished by neurotoxin sensitivity. *Nat. Neurosci.* 1:192–200. http://dx.doi.org/10.1038/642

Yu, X., K.L. Duan, C.F. Shang, H.G. Yu, and Z. Zhou. 2004. Calcium influx through hyperpolarization-activated cation channels (I(h) channels) contributes to activity-evoked neuronal secretion. *Proc. Natl. Acad. Sci. USA.* 101:1051–1056. http://dx.doi.org/10.1073/pnas.0305167101

Zeilhofer, H.U., M. Kress, and D. Swandulla. 1997. Fractional Ca^{2+} currents through capsaicin- and proton-activated ion channels in rat dorsal root ganglion neurones. *J. Physiol.* 503:67–78. http://dx.doi.org/10.1111/j.1469-7793.1997.067bi.x

Zhang, C., and Z. Zhou. 2002. Ca^{2+}-independent but voltage-dependent secretion in mammalian dorsal root ganglion neurons. *Nat. Neurosci.* 5:425–430.

Zhou, Z., and E. Neher. 1993. Mobile and immobile calcium buffers in bovine adrenal chromaffin cells. *J. Physiol.* 469:245–273. http://dx.doi.org/10.1113/jphysiol.1993.sp019813

Zurborg, S., B. Yurgionas, J.A. Jira, O. Caspani, and P.A. Heppenstall. 2007. Direct activation of the ion channel TRPA1 by Ca^{2+}. *Nat. Neurosci.* 10:277–279. http://dx.doi.org/10.1038/nn1843